Harmonic Axisymmetric Thick Shell Element for Static and Vibration Analyses

Jin-Gon Kim*

School of Mechanical and Automotive Engineering, Catholic University of Daegu, Hayang-up, Kyungsan-si, Kyongbuk, 712-702, Korea

In this study, a new harmonic axisymmetric thick shell element for static and dynamic analyses is proposed. The newly proposed element considering shear strain is based on a modified Hellinger-Reissner variational principle, and introduces additional nodeless degrees for displacement field interpolation in order to enhance numerical performance. The stress parameters selected via the field-consistency concept are very important in formulating a trouble-free hybrid-mixed elements. For computational efficiency, the stress parameters are eliminated by the stationary condition and then the nodeless degrees are condensed out by the dynamic reduction. Several numerical examples confirm that the present element shows improved efficiency and yields very accurate results for static and vibration analyses.

Key Words: Harmonic Axisymmetric Shell Element, Hybrid-Mixed Formulation, Static and Vibration Analyses

1. Introduction

Axisymmetric shells are common structural elements and are found in many areas of engineering. Their use includes pressure vessels, cooling towers, wheels, tires and turbine engine components, which spans all branches of engineering. Compared to a beam or plate, a shell may be considered as a thin structural element with double curvature. The curvature has a very significant effect on the behavior of a structure in carrying loads. At the same time, it introduces complexity into the formulation and numerical calculation. Thus the development of suitable finite elements for shells of revolution has been the subject of intensive research interest. Up till now, many techniques on a displacement-based element have been proposed including the selective/reduced integration element method (Zienkiewicz et al., 1977 ; Noor and Peters, 1981 ; Stolarski and Belytschko, 1983), the anisoparametric interpolation element method (Tessler and Spiridigliozzi, 1988), the strain-based element (Ryu and Sin, 1996), and the field-consistent element method (Prathap and Ramesh Babu, 1986 ; Ramesh Babu and Prathap, 1986). As an alternative to the displacement-based elements, the mixed or hybrid-mixed finite element method, which is the Hellinger-Reissner variational principle, has been continuously developed (Saleeb and Chang, 1987 ; Kim and Kim, 1996 ; Kim and Kim, 2000 ; Kim and Kang, 2003).

In the present work, a new and more accurate hybrid-mixed C^0 harmonic axisymmetric shell element for static and vibration analysis is presented based on the modified Hellinger-Reissner variational principle (Steele and Kim, 1993). A conventional Hellinger-Reissner variational principle for general shells has five displacements and eight stress resultants, but the modified Hellinger-Reissner variational principle employed in this work has only five displacements and five stress resultants ; the circum-

* **E-mail** : kimjg1@cu.ac.kr
TEL : +82-053-850-2711; **FAX** : +82-053-850-2710
School of Mechanical and Automotive Engineering, Catholic University of Daegu, Hayang-up, Kyungsan-si, Kyongbuk, 712-702, Korea. (Manuscript **Received** March 4, 2004; **Revised** June 10, 2004)

ferential stress resultants that cannot be prescribed at the shell edge are removed at the final form of the modified principle. In addition to the interpolating functions associated with nodal displacements and stress parameters, this element uses bubble functions corresponding to nodeless displacement degrees of freedom. The introduction of the nodeless degrees and the consistent stress parameters serves to greatly improve numerical results for bending responses and higher vibration modes, as well as to remove the locking phenomena. For computational efficiency, the stress parameters are substituted by the displacement variables at the element level. Furthermore, the additional nodeless degrees of freedom are also eliminated in the element equation of motion through the Guyan reduction (Guyan, 1965), and thus the number of the final system equations is greatly reduced.

Slightly increased computational efforts due to the use of the nodeless degrees of freedom are needed at the element level. However, these efforts can be well compensated by the substantially improved performance. Several numerical examples show that the present element yields very accurate results for the static and free vibration analysis of various axisymmetric shell problems.

2. Variational Principle

The meridional curvature and the normal component of the circumferential curvature are denoted by $1/r_1=d\varphi/ds$ and $1/r_2=\sin\varphi/r$ respectively, and the arc-length of the meridian of the mid-surface is expressed by s (Fig. 1). The tangential displacements, u and v, are in s and θ directions respectively, while w is the normal deflection. By assuming that the normal deflection is constant across the thickness of the shell, i.e., in ς direction shown in Fig. 2, the displacements are taken to be in the form of

$$\mathbf{U}=\begin{Bmatrix} w \\ u \\ v \end{Bmatrix}=\begin{Bmatrix} u_n \\ u_s+\varsigma\chi_s \\ u_\theta+\varsigma\chi_\theta \end{Bmatrix}, \tag{1}$$

where u_n is the measure of the normal deflection of the mid-surface, and u_s and u_θ indicate displacements at the mid-surface in s and θ directions respectively. χ_s and χ_θ are the measures of the rotation of the normal to the mid-surface.

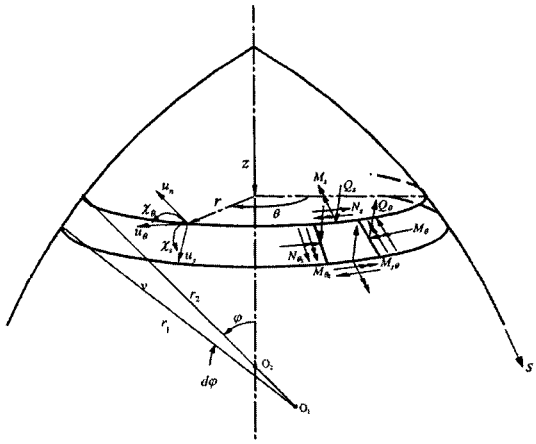

Fig. 1 Geometry of an axisymmetric shell

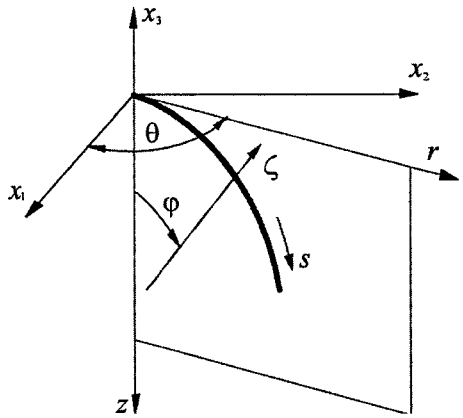

Fig. 2 The three-dimensional view of the r-z plane containing a meridian with arc length s and an outward normal ς. The angle φ is measured from the axis of revolution to the normal

Assuming time-harmonic motion with the natural angular frequency ω and integrating the variation of the kinetic energy over the volume at a fixed time, the Modified Hellinger-Reissner functional for axisymmetric shell can be written as

$$\delta\Pi_R=\delta\left\{\int_0^{2\pi}\left[\int_{s_1}^{s_2}L_R ds-\frac{1}{2}\rho\omega^2\int_{s_1}^{s_2}\int_{-t/2}^{t/2}\mathbf{U}^t\cdot\mathbf{U}dhds\right]rd\theta\right\}=0, \tag{2}$$

where ρ is the mass density and L_R is the energy density (refer to the reference (Kim and Kim,

2001) for the details). It is possible to write the energy density only in terms of the quantities that can be prescribed at the shell edges, namely the displacement vector $\mathbf{D}$ and the stress resultant vector $\mathbf{F}$ defined as

$$\mathbf{D}=\begin{Bmatrix}\chi_s\\ \chi_\theta\\ u_n\\ u_s\\ u_\theta\end{Bmatrix}=\begin{Bmatrix}\chi_s^{(n)}\cos n\theta\\ \chi_\theta^{(n)}\sin n\theta\\ u_n^{(n)}\cos n\theta\\ u_s^{(n)}\cos n\theta\\ u_\theta^{(n)}\sin n\theta\end{Bmatrix};\qquad \mathbf{F}=\begin{Bmatrix}M_s\\ M_{s\theta}\\ Q_s\\ N_s\\ N_{s\theta}\end{Bmatrix}=\begin{Bmatrix}M_s^{(n)}\cos n\theta\\ M_{s\theta}^{(n)}\sin n\theta\\ Q_s^{(n)}\cos n\theta\\ N_s^{(n)}\cos n\theta\\ N_{s\theta}^{(n)}\sin n\theta\end{Bmatrix}, \tag{3}$$

in which the quantities superscribed with n are the Fourier coefficients of the nth circumferential harmonic. The variation with respect to the circumferential angle, θ, can be integrated over the circumference, and then the circumferential harmonics are all uncoupled. Thus, integrating $\delta\Pi_R$ over θ, the final form of the modified mixed variational principle for the nth circumferential harmonic becomes

$$\delta\Pi_R^{(n)}=\delta\left\{k\pi\left[\int_{s_1}^{s_2}L_{MR}^{(n)}ds-\frac{1}{2}\rho\omega^2\int_{s_1}^{s_2}\int_{-t/2}^{t/2}\mathbf{D}^{(n)t}\mathbf{T}^t\mathbf{T}\mathbf{D}^{(n)}dhrds\right]\right\}=0$$

$$k=2 \text{ for } n=0,\ k=1 \text{ for } n>1 \tag{4}$$

The modified energy density $L_{MR}^{(n)}$ for the nth harmonic is given as

$$L_{MR}^{(n)}=\mathbf{F}^{(n)t}\cdot\frac{d\mathbf{D}^{(n)}}{ds}+\mathbf{D}^{(n)t}\cdot\mathbf{E}^{(n)}\cdot\mathbf{F}^{(n)}-\frac{1}{2}\mathbf{F}^{(n)t}\cdot\mathbf{C}\cdot\mathbf{F}^{(n)}+\frac{1}{2}\mathbf{D}^{(n)t}\cdot\mathbf{K}^{(n)}\cdot\mathbf{D}^{(n)} \tag{5}$$

The symmetric matrices $\mathbf{C}$ and $\mathbf{K}^{(n)}$ have dimensions of "compliance" and "stiffness" repectively. For isotropic materials, the matrices $\mathbf{E}^{(n)}$, $\mathbf{C}$, and $\mathbf{K}^{(n)}$ are explicitly given in Appendix.

3. Finite Element Formulation

In the present 3-noded finite element formulation, the displacement field variables (χ_s, χ_θ, u_n, u_s, u_θ) are interpolated using the bubble function such as $\xi(1-\xi^2)$ in addition to the familiar quadratic Lagrangian polynomials. The dimensionless parameter varies from 0 to 1 in an element and is defined as $ds=(r_\xi^2+z_\xi^2)^{1/2}d\xi=|J|d\xi$. The purpose of using the nodeless degrees is to describe the bending behavior and higher-order vibration modes of axisymmetric shells more accurately. Thus, the displacements $\mathbf{D}^{(n)}$ in Eq. (5) within an element are interpolated as

$$\mathbf{D}^{(n)}=[\mathbf{N}_c:\mathbf{N}_h]\cdot\{\mathbf{d}_c^{(n)},\mathbf{d}_h^{(n)}\}^t=\mathbf{N}\cdot\mathbf{d}^{(n)}, \tag{6}$$

where $\mathbf{N}_c$ and $\mathbf{N}_h$ denote the matrices representing the interpolation functions for the nodal $\mathbf{d}_c^{(n)}=\{\chi_{si},\chi_{\theta i},u_{ni},u_{si},u_{\theta i}\}_{i=1,3}^t$ and nodeless $\mathbf{d}_h^{(n)}=\{a_i\}_{i=1,5}^t$ degrees of freedom respectively.

As the shell becomes extremely thin and nearly straight, the membrane and shear strains must vanish in the limits of membrane inextensibility and shearless deformation. These constraints yield unnecessary restrictions expressed by $u_{u,\xi\xi\xi}\to 0$ and $\chi_{s,\xi\xi\xi}\to 0$ at the element level. These are known as spurious constraints which lead to membrane and shear locking. To remove the spurious constraints, the stress resultants corresponding to troublesome strains should be consistent quadratic interpolation functions. Therefore, the following form of stress interpolation functions is employed.

$$\mathbf{F}^{(n)}=\mathbf{S}(1,\xi,\xi^2)\cdot\boldsymbol{\beta}^{(n)}, \tag{7}$$

where $\boldsymbol{\beta}^{(n)}=\{\beta_1,\ldots,\beta_{15}\}$, denoting the stress parameters for the nth harmonic number, are not continuous at the element boundary, and $\mathbf{S}$ is the matrix of the interpolation functions for stress resultants.

The present hybrid-mixed element employing Eqs. (6) and (7) is designated by DCSQ3. This element is compared with a hybrid-mixed element DQSL3 (Kim and Kim, 1996) with quadratic-displacement and consistent linear-stress resultant interpolation functions. A hybrid-mixed element DCSC3 with cubic-displacement in Eq. (6) and inconsistent cubic-stress resultant interpolation is also compared with the present DCSQ3 element. These comparisons demonstrate the effects of the consistent stress parameters and nodeless degrees in hybrid-mixed formulation for static and vibration analyses. The characteristic of the elements compared in the present work are summarized in Table 1.

Table 1 The characteristics of the finite element models used in the present study

Displacement Approximation	Stress Approximation	Designation	Consistency	Possible locking
Quadratic	-	DQ3	Inconsistent	Yes
Quadratic	Quadratic	DQSQ3	Inconsistent	Yes
Quadratic	Linear	DQSL3	Consistent	No
Cubic	Quadratic	DCSQ3 (present)	Consistent	No

For the finite element formulation, the substitution of Eqs. (6) and (7) into equation (4) yields

$$\Pi_R^{(n)}=\boldsymbol{\beta}^{(n)t}\mathbf{G}\mathbf{d}^{(n)}+\mathbf{d}^{(n)t}\boldsymbol{\Xi}^{(n)}\boldsymbol{\beta}^{(n)}-\frac{1}{2}\boldsymbol{\beta}^{(n)t}\mathbf{I}\boldsymbol{\beta}^{(n)} +\frac{1}{2}\mathbf{d}^{(n)t}\boldsymbol{\Theta}^{(n)}\mathbf{d}^{(n)}-\frac{1}{2}\omega^2\mathbf{d}^{(n)t}\mathbf{M}^{(n)}\mathbf{d}^{(n)} \tag{8}$$

where

$$\mathbf{G}=\int_0^1[\mathbf{S}^t\cdot(\mathbf{N}_{c,\xi}:\mathbf{N}_{h,\xi})]\,r\,d\xi=(\mathbf{G}_c:\mathbf{G}_h) \tag{9a}$$

$$\boldsymbol{\Xi}^{(n)}=\int_0^1 r(\mathbf{N}_c:\mathbf{N}_h)^t\mathbf{E}^{(n)}\mathbf{S}|J|\,d\xi=(\boldsymbol{\Xi}_c^{(n)}:\boldsymbol{\Xi}_b^{(n)})^t \tag{9b}$$

$$\mathbf{I}=\int_0^1 r\mathbf{S}^t\mathbf{C}\mathbf{S}|J|\,d\xi \tag{9c}$$

$$\boldsymbol{\Theta}^{(n)}=\int_0^1 r(\mathbf{N}_c:\mathbf{N}_h)^t\mathbf{K}^{(n)}(\mathbf{N}_c:\mathbf{N}_h)|J|\,d\xi =(\boldsymbol{\Theta}_{ij}^{(n)})_{i,j=c,h} \tag{9d}$$

$$\mathbf{M}^{(n)}=\rho\int_0^1\int_{-t/2}^{t/2} r\mathbf{N}^t\mathbf{T}^t\mathbf{T}\mathbf{N}\,dh|J|\,d\xi \tag{9e}$$

By invoking the stationarity of $\Pi_R^{(n)}$ with respect to $\mathbf{d}^{(n)}$ and $\boldsymbol{\beta}^{(n)}$ respectively, and then applying the Guyan reduction, the following reduced eigenvalue problem for free-vibration analysis, which is expressed only in terms of $\mathbf{d}_c^{(n)}$, can be obtained.

$$[\mathbf{K}_e^{(n)}-\omega^2\mathbf{M}_e^{(n)}]\mathbf{d}_e^{(n)}=0, \tag{10}$$

where the condensed element stiffness matrix $\mathbf{K}_e^{(n)}$ and mass matrix $\mathbf{M}_e^{(n)}$ are given by

$$\mathbf{K}_e^{(n)}=\mathbf{K}_{cc}^{(n)}-\mathbf{K}_{ch}^{(n)}\mathbf{K}_{hh}^{(n)^{-1}}\mathbf{K}_{hc}^{(n)} \tag{11a}$$

$$\mathbf{M}_e^{(n)}=\mathbf{M}_{cc}^{(n)}+\mathbf{K}_{ch}^{(n)}\mathbf{K}_{hh}^{(n)^{-1}}\mathbf{M}_{hh}^{(n)}\mathbf{K}_{hh}^{(n)^{-1}}\mathbf{K}_{hc}^{(n)}- \mathbf{K}_{ch}^{(n)}\mathbf{K}_{hh}^{(n)^{-1}}\mathbf{M}_{hc}^{(n)}-\mathbf{M}_{ch}^{(n)}\mathbf{K}_{hh}^{(n)^{-1}}\mathbf{K}_{hc}^{(n)}, \tag{11b}$$

where

$$\mathbf{K}_{ij}^{(n)}=(\mathbf{G}_i^t+\boldsymbol{\Xi}_i^{(n)})\mathbf{I}^{-1}(\mathbf{G}_j+\boldsymbol{\Xi}_j^{(n)t})+\boldsymbol{\Theta}_{ij}^{(n)} \quad (i \text{ and } j=\text{c, h}) \tag{12a}$$

$$\mathbf{M}_{ij}^{(n)}=\rho\int_0^1\int_{-t/2}^{t/2} r\mathbf{N}_i^t\mathbf{T}^t\mathbf{T}\mathbf{N}_j\,dh|J|\,d\xi \quad (i \text{ and } j=\text{c, h}) \tag{12b}$$

4. Numerical Examples

In this section, the results by the present DCSQ3 element are compared with those reported in literatures for evaluating the numerical performance for the static and free vibration analyses.

4.1 Ring-loaded cantilever pipe

Fig. 3 shows a cantilever circular cylindrical shell under an axisymmetric tip load (1 lbf/in) along the free edge (Prathap and Ramesh Babu, 1986). This problem has an interesting constraint such that the equation of equilibrium for the in-plane force reduces to $N_{s,s}=0$. Most axisymmetric

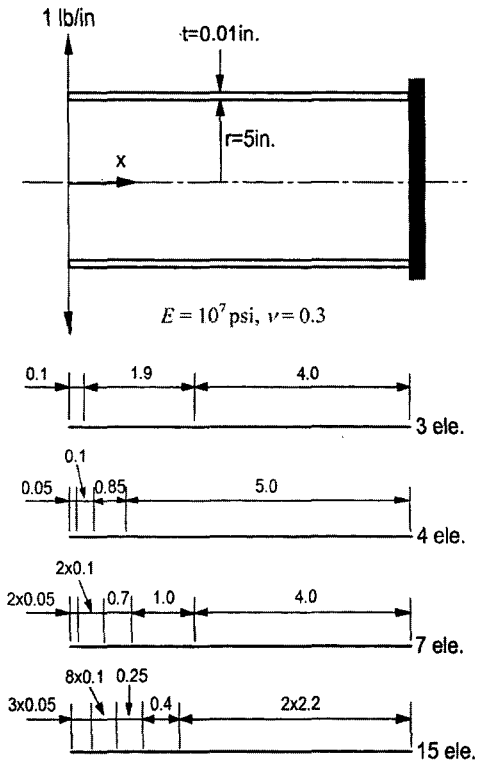

Fig. 3 Cantilever circular cylindrical shell and its nodal division

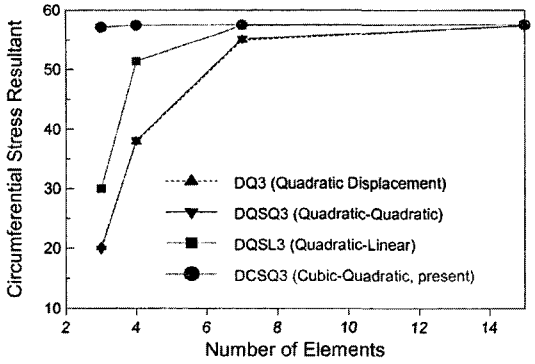

Fig. 4 Convergence behavior for the circumferential stress resultant at the free edge of ring-loaded cantilever pipe.

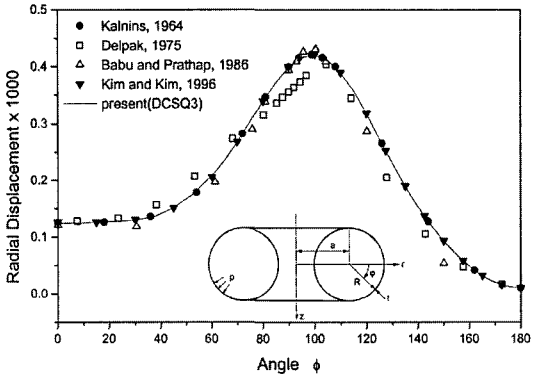

Fig. 5 The radial displacement distribution of a toroidal shell

shell elements cannot satisfy this constraint due to the inconsistency between ε_s and ε_θ. Four nodal divisions using 3, 4, 7 and 15 elements are also shown in Fig. 3.

Fig. 4 shows the convergence behavior for the circumferential stress resultant N_θ at the free edge. It is clear that the hybrid-mixed element DQSQ3 produces less accurate results due to its inconsistent stress approximation, and these results are equivalent to those by the standard displacement element DQ3. The DQSL3 element shows faster convergence than the DQSQ3 element. The DCSQ3 element requires some additional calculations to obtain $\mathbf{K}_{ch}^{(n)}\mathbf{K}_{hh}^{(n)-1}\mathbf{K}_{hc}^{(n)}$ in Eq. (11a) for each element. However, the results by the use of three DCSQ3 elements that requires only a 21-by-21 matrix manipulation in order to obtain the same accurate results as those from the use of seven DQSL3 elements that requires 45-by-45 matrix manipulation. It is clear that regardless of the additional computational effort needed for DCSQ3, DCSQ3 with the additional nodeless degrees is more effective than other elements such as DQSL3 in static analysis.

4.2 Toroidal shell under uniform internal pressure

A toroidal shell under internal pressure p in Fig. 5 is chosen to prove the ability of the present elements to predict the rapid change in membrane resultants. The material properties and shell dimensions are $E=10^7\text{lb/in}^2$, $\nu=0.3$, $t=0.5\text{in}$, $a=15\text{in}$, $R=10\text{in}$ and $p=1\text{lb/in}^2$. The shell meridian for $z>0$ is discretized by 7 unevenly spaced DCSQ3 elements, with more elements at the pole. The results are compared to Kalnins' direct numerical integration results (1964) and those by Delpak's curved parametric element (1975), Babu and Prathap's field-consistent element (1986), and Kim and Kim's hybrid-mixed element with consistent stress parameters (1996).

Fig. 5 compares the present result for the radial displacement u_r with those reported in the literatures. Fig. 6 shows the circumferential membrane resultant N_θ. Eleven DQSL3 elements are required to obtain the results comparable to Kalnins' result while only seven DCSQ3 elements are. We note that DCSQ3 and DQSL3 predict the membrane resultants better than Delpak's and Prathap's elements: compare these results with Kalnins' result in Fig. 6.

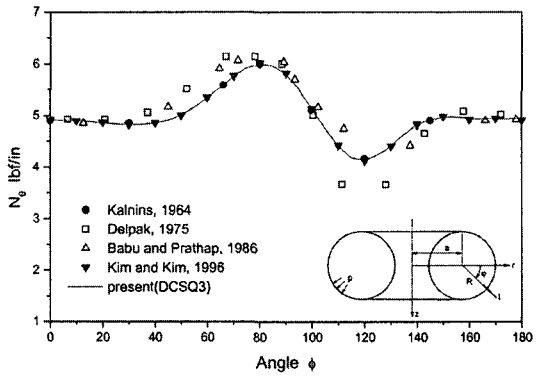

Fig. 6 The distribution of the circumferential stress resultant of a toroidal shell

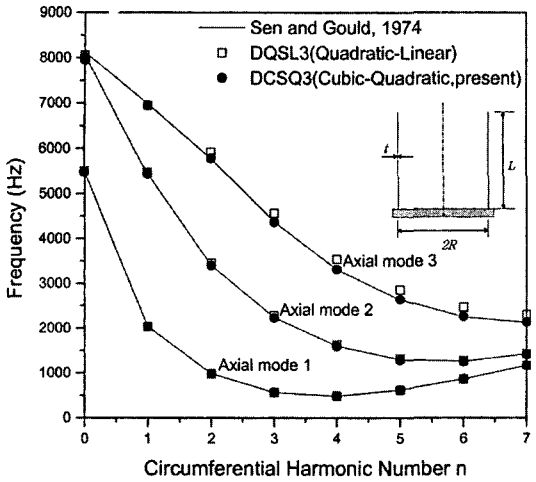

Fig. 7 Differences between two elements' results by DQSL3 and DCSQ3 and the Sen & Gould's results in the prediction of the natural frequencies of a clamped-free cylindrical shell for the circumferential wave number.

4.3 Clamped-free cylindrical shell

The first three natural frequencies of the clamped-free cylindrical shell in Fig. 7 are obtained. The shell dimensions and material properties are $R=101.6$mm, $L=226.786$mm, $t=1.016$mm, $E=2.069\times10^{11}$N/m^2, $\nu=0.3$, and $\rho=7868$kg/m^3.

The two-element results by DQSL3 and DCSC3 are compared in Fig. 7 with the results by Sen and Gould (1974) who used a displacement-based finite element technique. Their results were obtained with 6 to 12 elements depending on the harmonic number. A good agreement is seen between the two DCSQ3 element results and those by Sen and Gould. It should be noted that the adoption of higher-order interpolation functions and consistent stress parameters in the hybrid-mixed formulation yields substantially improved results for higher natural frequencies.

4.4 Clamped-free hyperbolic shell

The free vibration response of the hyperbolic shell as shown in Fig. 8 is considered. This problem was investigated numerically by Sen and Gould (1974) who used the finite element technique as well as experimentally by Hashish (1971) who used a scale model of a prototype

Table 2 Natural frequencies of the clamped-free hyperbolic shell depicted in Fig. 8

Harmonic Number n	Natural frequencies (Hz)			
	Experiment (Hashish, 1971)	Sen and Gould (1974)	DCSQ3 (6 elements)	DCSQ3 (8 elements)
3	188	168	167.51	167.52
4	130	130	129.86	129.83
5	-	122	122.19	122.16
6	157	143	143.10	142.86
7	177	161	161.82	161.30

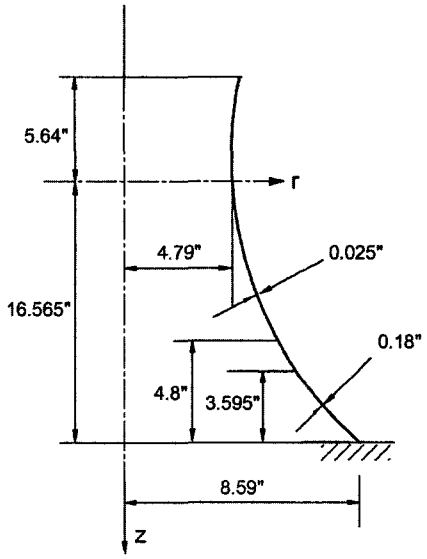

Fig. 8 A hyperbolic shell model.

hyperbolic cooling tower. A cross section is defined by the hyperbola equation, $(r/a)^2-(z/b)^2=1$, where $a=4.79$ and $b=11.391$. The material properties are $E=0.738\times10^6$psi, $\nu=0.3$, and $\rho=0.210\times10^{-3}$lbf/in^3. In the present analysis, the shell is assumed to be clamped at the base and free at the top, while all thickness variations are taken into consideration.

The results of the present results using six and eight elements are tabulated in Table 2 together with those obtained by Hashish (1971) and Sen & Gould (1974). It is seen from Table 2 that the experimental frequencies are consistently higher than those predicted by finite element analyses. This discrepancy may be attributed to the change in the mechanical properties of the model which

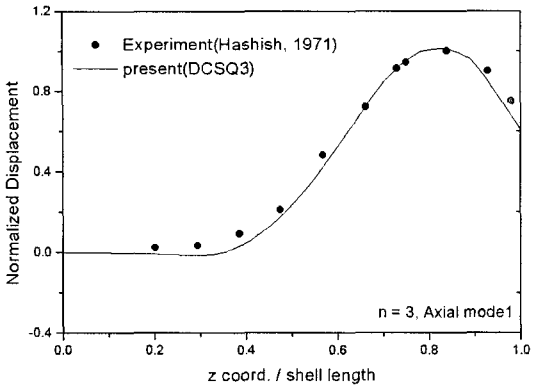

(a)

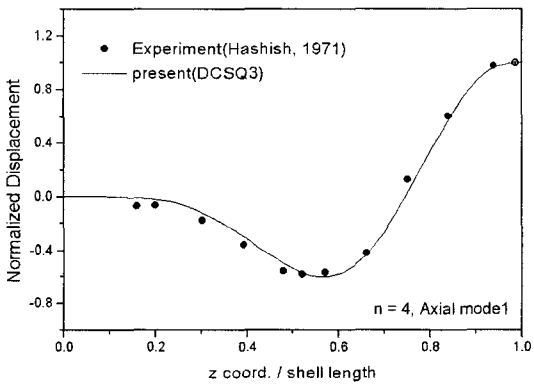

(b)

Fig. 9 First mode shapes for circumferential harmonic numbers, (a) $n=3$ and (b) $n=4$

have not been considered in the analysis, but well-converged results with fewer elements are obtained. Fig. 9 shows the mode shape for the circumferential harmonic number $n=3$ and $n=4$. It is evident that even with a small number of elements, the present DCSQ3 is capable of solving practical problems accurately.

5. Conclusions

In this study, the static and vibration analyses using a new harmonic axisymmetric shell element are performed. In developing the present elements, special efforts are exercised :

-to select suitable and straightforward interpolation functions for stress resultants to remove the spurious constraints by means of the field -consistent concept ;

-to improve the accuracy and convergence in the prediction for a bending behavior and higher-order vibration mode by introducing nodeless degrees.

It is confirmed that the introduction of additional nodeless degrees of freedom and consistent stress parameters is very effective in formulating trouble-free hybrid-mixed elements. Several numerical examples confirm the present element's superior performance for both the static and vibration analyses.

Appendix

The explicit form of the matrices $\mathbf{E}^{(n)}$, $\mathbf{C}$, and $\mathbf{K}^{(n)}$ are given by

$$\mathbf{E}^{(n)}=\begin{bmatrix} \nu\frac{c_\varphi}{r} & -\frac{n}{r} & 1 & 0 & 0 \\ \nu\frac{n}{r} & -\frac{c_\varphi}{r} & 0 & 0 & 0 \\ 0 & 0 & 0 & \frac{1}{r_1}+\nu\frac{s_\varphi}{r} & 0 \\ 0 & -\frac{2\zeta n}{r} & -\frac{1}{r_1} & \nu\frac{c_\varphi}{r} & -\frac{n}{r} \\ 0 & -\frac{2\zeta c_\varphi}{r} & 0 & \nu\frac{n}{r} & -\frac{c_\varphi}{r} \end{bmatrix} \tag{A.1}$$

$$\mathbf{K}^{(n)}=\frac{Et}{r^2}\begin{bmatrix} \frac{c_\varphi^2 t^2}{12} & \frac{nc_\varphi^2 t}{12} & 0 & 0 & 0 \\ \frac{nc_\varphi^2 t^2}{12} & \frac{n^2 t^2}{12}+\frac{r^2}{\mu} & -\frac{nr}{\mu} & 0 & -\frac{rs_\varphi}{\mu} \\ 0 & -\frac{nr}{\mu} & \frac{n^2}{\mu}+s_\varphi^2 & s_\varphi c_\varphi & ns_\varphi\left(1+\frac{1}{\mu}\right) \\ 0 & 0 & s_\varphi c_\varphi & c_\varphi^2 & nc_\varphi \\ 0 & -\frac{rs_\varphi}{\mu} & ns_\varphi\left(1+\frac{1}{\mu}\right) & nc_\varphi & \frac{s_\varphi^2}{\mu}+n^2 \end{bmatrix} \tag{A.2}$$

$$\mathbf{C}=\frac{1}{Et}=\begin{bmatrix} \frac{1}{c^2} & 0 & 0 & 0 & 0 \\ 0 & \frac{2}{c^2(1-\nu)}+2\zeta^2(1+\nu) & 0 & 0 & 2\zeta(1+\nu) \\ 0 & 0 & \mu & 0 & 0 \\ 0 & 0 & 0 & 1-\nu^2 & 0 \\ 0 & 2\zeta(1+\nu) & 0 & 0 & 2(1+\nu) \end{bmatrix} \tag{A.3}$$

with

$$s_\varphi=\sin\varphi\,;\ c_\varphi=\cos\varphi.$$

In Eqs. (A.1)~(A.3), E and ν are Young's modulus and Poisson's ratio, respectively, the

shear flexibility factor μ and the reduced thickness c are taken to be given by

$$\mu=\frac{12(1+\nu)}{5}\ ;\ c^2=\frac{t^2}{12(1-\nu^2)}\ .$$

References

Delpak, R., 1975, "Role of the Curved Parametric Element in Linear Analysis of Thin Rotational Shells," *Ph. D. Thesis*, Department of Civil Engineering, Polytechnic of Wales.

Guyan, R. J., 1965, "Reduction of Stiffness and Mass Matrices," *American Institute of Aeronautics and Astronautics Journal*, Vol. 3, pp. 380

Hashish, M. G. and Abu-Sitta, S. H., 1971, "Free Vibration of Hyperbolic Cooling Towers," *American Society of Civil Engineers Journal*, Vol. 97, pp. 253~269

Kalnins, A., 1964, "Analysis of Shells of Revolution Subjected to Symmetrical and Nonsymmetrical Loads," Journal of Applied Mechanics, Vol. 31, pp. 467~476

Kim, J. G. and Kang, S. W., 2003, "A New and Efficient Laminated Curved Beam Element," *Transactions of the KSME*, A, Vol. 27, No. 4, pp. 559-566.

Kim, J. G. and Kim, Y. Y., 2000, "A Higher-Order Hybrid-Mixed Harmonic Shell-of-Revolution Element," *Computer Methods for Applied Mechanics and Engineering*, Vol. 182, pp. 1~16

Kim, Y. Y. and Kim, J. G., 1996, "A Simple and Efficient Mixed Finite Element for Axisymmetric Shell Analysis," *International Journal of Numerical Methods for Engineering*, Vol. 39, pp. 1903~1914

Noor, A. K. and Peters, J. M., 1981, "Mixed and Reduced/Selective Integration for Curved Elements," *International Journal for Numerical Methods in Engineering*, Vol. 17, pp. 615~631

Prathap, G. and Ramesh Babu, C., 1986, "A Field-Consistent Three-Noded Quadratic Curved Axisymmetric Shell Element," *International Journal for Numerical Methods in Engineering*, Vol. 23, pp. 711~723

Ramesh Babu, C. and Prathap, G., 1986, "A Field-Consistent Two-Noded Curved Axisymmetric Shell Element," International Journal for Numerical Methods in Engineering, Vol. 23, pp. 1245~1261

Ryu, H. S. and Sin, H. C., 1996, "A 2-Node Strain Based Curved Beam Element," *Transactions of the KSME*, Vol. 18, No. 8, pp. 2540~2545.

Saleeb, A. F. and Chang, T. Y., 1987, "On the Hybrid-Mixed Formulation Curved Beam Elements," *Computer Methods in Applied Mechanics and Engineering*, Vol. 60, pp. 95~121.

Sen, S. K. and Gould, P. L., 1974, "Free Vibration of Shells of Revolution Using FEM," *American Society of Civil Engineers Journal*, Vol. 100, pp. 283~303

Steele, C. R. and Kim, Y. Y., 1993, "Modified Mixed Variational Principle and the State-Vector Equation for Elastic Bodies and Shells of Revolution," *Journal of Applied Mechanics*, Vol. 59, pp. 587~595

Stolarski, H. and Belytschko, T., 1983, "Shear and Membrane Locking in Curved C0 Elements," *Computer Methods in Applied Mechanical Engineering*, Vol. 41, pp. 279~296

Tessler, A. and Spiridigliozzi, L., 1988, "Resolving Membrane and Shear Locking Phenomena in Curved Shear-Deformable Axisymmetric Shell Element," *International Journal for Numerical Methods in Engineering*, Vol. 26, pp. 1071~1086

Zienkiewicz, O. C., Bauer, J., Morgan, K. and Onate, E., 1977, "A Simple and Efficient Element for Axisymmetric Shells,". *International Journal for Numerical Methods in Engineering*, Vol. 11, pp. 1545~1558